LINEAR LATTICE FOR THE LSB STORAGE RING

Marc Muñoz,
Laboratori del Sincrotro de Barcelona-IFAE, E-08193 Barcelona, Spain

Abstract

The LSB will be a third generation light source working at an energy of 2.5 GeV. The machine is composed of 12 identical cells with a total circumference around 250 meters. The lattice chosen is a TBA with a quadrupolar component in the bending magnets. This lattice provides a low emittance and offers good potential for future upgrades (higher energy, use of superconducting dipoles). In this paper we describe the linear lattice used and discuss other issues, such as closed orbit correction, emittance coupling control, and upgrading the machine by replacing the central dipole of some cells with superconducting ones.

1 DESIGN REQUIREMENTS

The aim of the design [1] is to provide a lattice with low emittance (under 10 πnm-rad), a critical photon energy in the range of 4 to 5 keV, and at least nine straight sections for insertion devices, with a total circumferece of the machine under 250 meters. The lattice that fulfils the design requirements is a TBA lattice with gradient in the bending with 12 cell.

The lattice chosen is shown in Figure 1. The cell is composed by a quadrupole doublet in the dispersion free region, and an achromat with three identical combined function magnets (with dipolar and quadrupolar field), with a quadrupole between each pair.

The dipolar field of the bending magnets is 1 Tesla, chosen to provide a critical energy of the photons of 4.2 keV. The magnets have the potential to reach a field of 1.2 Tesla, providing potential for future upgrades of the machine to higher energy.

2 BASIC PARAMETERS

The strength of the quadrupole Q1 is selected to vanish the horizontal dispersion at the extremes of the achromat. The strength of the quadrupoles QF and QD are used to select the desired working , Q_x=14.2, Q_y=8.3. This point offers a low emittance and chromaticity, and would provide a large dynamic aperture.

The Table 1 shows the main parameters of the machine. The optical functions for one cell are shown in Figure 2. The electron beam sizes along the machine are shown in Figure 3.

Table 1: Machine Parameters.

Lattice type	TBA	
Energy	2.5	GeV
Number of Cells	12	
Cell Length	20.987	m
Circumference	251.844	m
Q_x	14.20	
Q_y	8.30	
Equilibrium Emittance	8.35	nm-rad
Coupling	5%	
Horizontal Emittance	7.9	nm-rad
Vertical Emittance	0.45	nm-rad
Relative Energy Spread	8.61×10^{-4}	
Energy Lost per Turn	0.42	MeV
J_x	1.50	
J_y	1.00	
J_e	1.50	
τ_x	6.72	ms
τ_y	10.07	ms
τ_ε	6.71	ms
α_p	1.9×10^{-3}	
Critical Energy	4.20	keV
Harmonic number	420	
RF Frequency	500	MHz

This lattice satisfies all the requirements of the design, and, as we will show later, offers a low sensibility to errors and a low coupling.

3 SENSITIVITY TO ERRORS

An important aspect in any light source is the stability of the electron beam. The sensitivity of the machine to magnet errors should be as small as possible. The effect of the dipolar errors on the closed orbit is given, in the linear approximation, by:

$$\Delta x(s) = \frac{\sqrt{\beta(s)}}{4\sin Q}\sqrt{\sum_{errors}\beta(s_e)\frac{\Delta Bl}{B\rho}} \qquad (1)$$

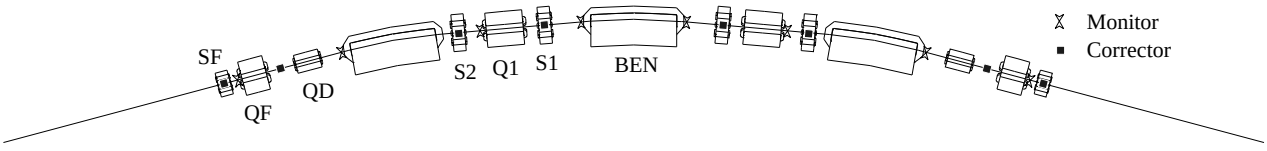

Figure 1: Layout of the cell.

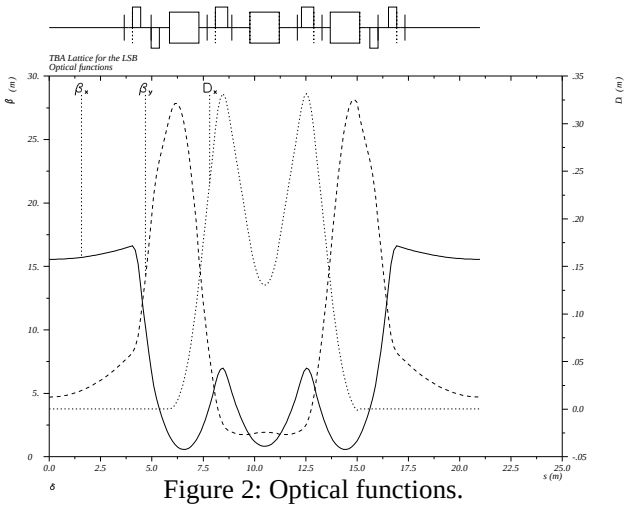

Figure 2: Optical functions.

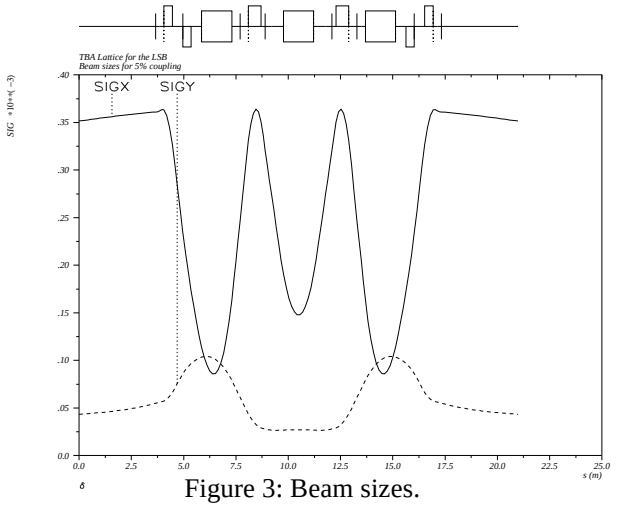

Figure 3: Beam sizes.

The closed orbit distortion has been modelled with MAD [2], BETA [3] and COUPXY [4], assuming the following errors:

- Transverse misalignment of magnets $\Delta x,y=0.1$ mm
- Roll angle misalignment of the quads $\Delta\theta=5\times10^{-4}$ rad
- Field imperfections in the dipoles $\Delta B/B_0=5\times10^{-4}$

The average values of the rms and maximum closed orbit error have been found of:

	Horizontal	Vertical
rms	4 mm	8 mm
maximum	7.5 mm	12 mm

3.1 Correction System

The Figure 1 shows scheme used to compensate the closed orbit distortion. Some correctors are included in the sextupoles, while others are separate magnets. We use 8 monitors per cell. All the monitors and the correctors operate in both planes.

The effect of the correction system has been simulated with MAD and COUPXY. Both programs agreed in the results. Figures 4 and 5 show the maximum closed orbit displacement in both planes, before and after correction, for 100 sample machines. Figure 6 shows the distribution of the maximum corrector strength.

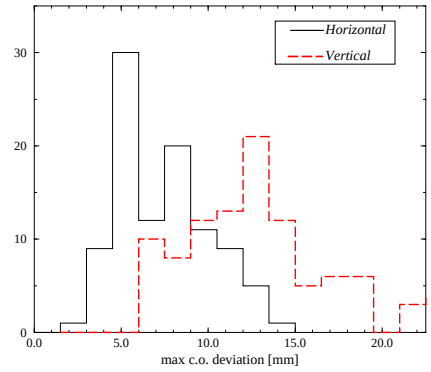

Figure 4: Closed orbit distortion before correction.

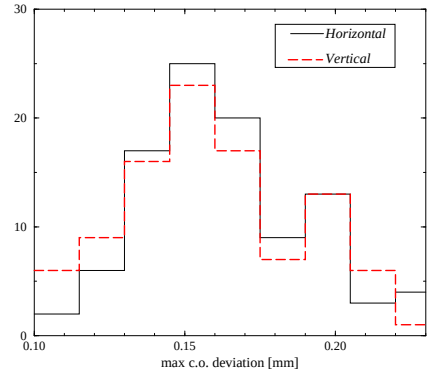

Figure 5: Closed orbit distortion after correction.

The closed orbit deviation has been corrected to a maximum value of 0.15 mm on average, with a maximum corrector strength of 0.5 mrad.

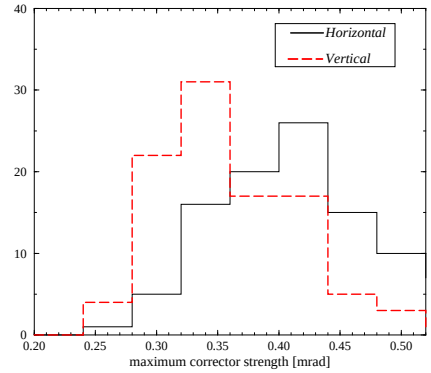

Figure 6: Distribution of maximum corrector strength.

3.2 Local Bumps

The correctors used for orbit correction can be used to provide user defined bumps in the insertion devices and bending magnets. A maximum deflection of 1.5 mrad in the correctors, will allow us to move the orbit up to 3 mm in the insertion devices.

4 COUPLING

One of the parameters that affect the most the performance of a light source is the coupling between the horizontal and vertical emittance:

$$\chi = \frac{\varepsilon_y}{\varepsilon_x} \tag{2}$$

Two are the factors that determine the emittance coupling:

•The vertical emittance due to the vertical dispersion generated by closed orbit errors [5].

$$\chi = \frac{J_x}{J_y}\frac{\langle \mathcal{H}_y \rangle}{\langle \mathcal{H}_x \rangle} \approx \frac{J_x}{J_y}\frac{\left\langle D^2{}_y / \beta_y \right\rangle}{\left\langle D^2{}_x / \beta_x \right\rangle}\Bigg|_{bending} \tag{3}$$

•The coupling between the horizontal and vertical plane generated by skew quadrupolar field and closed orbit errors in sextupoles [5].

$$\chi = \frac{\left|\kappa/\Delta\right|^2}{\left|\kappa/\Delta\right|^2 + 1/2} \tag{4}$$

$$\kappa = \frac{1}{4\pi}\oint K_s(s)\sqrt{\beta_x \beta_y}\,\exp\left[i\left(\mu_x - \mu_y - s\Delta/R\right)\right]ds$$

where K_s is $2K\Delta\theta$ for quadrupole rotation and $K_2\Delta y$ for orbit error in the sextupoles.

Using the values of the errors found in the previous section and the correction system already described, the values of the coupling found theoretically and using MAD and COUPXY are:

χ_{theory}=1.2 %

χ_{COUPXY}=1.0 %

χ_{MAD}=1.1 %

5 EFFECT OF THE INSERTION DEVICES

The insertion devices used to generate synchrotron light would affect the achieved emittance and energy dispersion. Figures 7 and 8 show the relative variation of the emittance and the energy dispersion for a typical wiggler and a typical undulator, of period 9.5 cm and 6 cm respectively, wiht a total length of 6 meters, as a function of the field and the number of devices.

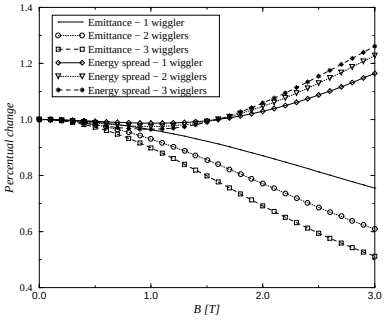

Figure 7: Effect of wigglers.

6 POSSIBLE UPGRADES

A possible future upgrade of the basic machine is the inclusion of superconducting dipoles replacing some of the central dipoles. The Figure 9 shows the increase of the emittance with the inclusion of a different number of 4 Tesla superconducting magnets.

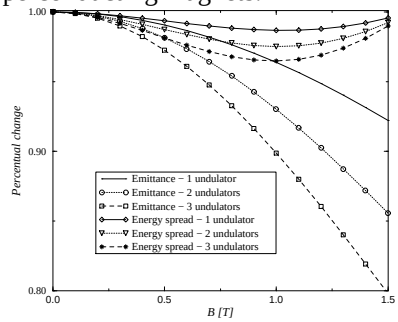

Figure 8. Effect of undulators.

Another possible upgrade is the increase of the machine energy to 3 GeV, increasing the critical energy up to 5 keV, but increassing the emittance to 12 nm-rad.

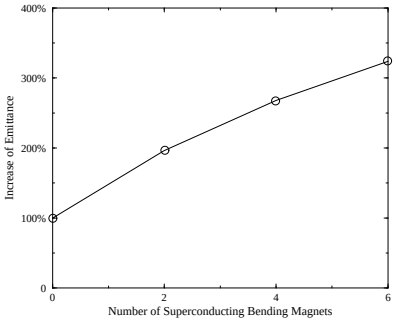

Figure 9. Effect of superconducting dipoles.

7 CONCLUSIONS

The lattice presented here shows a good potential as a 3rd generation light source. It offers low sensitivity to errors and a low coupling, while providing the opportunity of futures upgrades.

ACKNOWLEDGES

This work is supported by CIRIT and CICYT. I agree the helpful collaboration of the Accelerator Physics group of Daresbury Laboratory.

BIBLIOGRAPHY

[1]'The Spanish Project for a Synchrotron Laboratory at Barcelona', J. Bordas, this proceedings.

[2]'The MAD Program', C. Iselin et alt., CERN/SL/90-13 (AP)

[3]'BETA User's Guide', L. Farvacque et alt., ESRF-SR/LAT-88-08.

[4]'Two-Dimensional Analytical Coupling Code COUPXY', C. Prior, RAL

[5]'Horizontal-Vertical Coupling in the ESRF Storage Ring', C.W.Planner, C.R.Prior, COLL/RAL/ESRF-05/R06.